

## Measurements of low-energy neutral hydrogen efflux during ICRF heating

This article has been downloaded from IOPscience. Please scroll down to see the full text article.

1984 Nucl. Fusion 24 1490

(<http://iopscience.iop.org/0029-5515/24/11/009>)

View [the table of contents for this issue](#), or go to the [journal homepage](#) for more

Download details:

IP Address: 130.126.32.13

The article was downloaded on 25/12/2012 at 21:30

Please note that [terms and conditions apply](#).

## MEASUREMENTS OF LOW-ENERGY NEUTRAL HYDROGEN EFFLUX DURING ICRF HEATING

S.A. COHEN, D. RUZIC\*, D.E. VOSS\*\*, R. BUDNY, P. COLESTOCK, D. HEIFETZ, J. HOSEA, D. HWANG, D. MANOS, J. WILSON (Plasma Physics Laboratory, Princeton University, Princeton, New Jersey, United States of America)

**ABSTRACT.** Using the Low Energy Neutral Atom Spectrometer, measurements were made of the  $H^0$  and  $D^0$  efflux from PLT during ion cyclotron heating experiments. The application of RF power at frequencies appropriate to fundamental and second-harmonic heating results in a rapid, toroidally uniform rise in the charge-exchange efflux at a rate of about  $10^{15} \text{ cm}^{-2} \cdot \text{s}^{-1} \cdot \text{MW}^{-1}$ . This flux increase is larger at lower plasma currents. The cause of this flux and its impact on plasma behaviour are discussed.

The heating of hydrogen plasmas by the application of radio-frequency power in the ion cyclotron range of frequencies (ICRF) is being studied on the PLT tokamak. The experiments, which are aimed at achieving thermonuclear temperatures, include investigations of heating efficiency versus ICRF mode, plasma parameters, and antennae configurations [1]. Methods to diagnose and control the edge of the heated plasmas are important in these experiments in that deleterious processes may be avoided. Spectroscopic studies during low-power ICRF heating experiments performed on the ATC [2] and PLT [3] tokamaks showed a decrease in the edge ion temperature accompanying efficient ion heating in the plasma core. This edge cooling was proposed [3] as a new approach to avoid the influx of detrimental high-Z impurities. It was speculated that an influx of low-Z impurities caused radiative cooling of the edge plasma and, therefore, reduced sputtering of wall and limiter material. The origin of these impurities could well depend on limiter or antenna configurations and materials. In this letter, we report studies of edge processes in plasmas heated with higher levels of ICRF power and with a range of plasma currents. The observations have been made with different diagnostics which shed additional light on the processes involved.

One diagnostic that has special utility in characterizing the edge of ICRF-heated plasmas is the Low Energy Neutral Atom Spectrometer (LENS) [4]. This novel device, a time-of-flight spectrometer, detects hydrogen (or deuterium) atoms that are emitted from the plasma by neutralization processes, the main one of which is charge exchange. Because of the LENS's sensitivity [5] to particles with energies as low as 5 eV, it may be used to study edge plasma behaviour. In addition to the LENS, Langmuir probes [6] were used to monitor the plasma outside the limiter radius.

In these experiments the PLT toroidal magnetic field,  $B_T$ , was chosen to place the appropriate cyclotron resonance of the desired ion on the PLT magnetic axis. The two RF frequencies available for these experiments were 25 and 42 MHz. The lower frequency was used for the  $^3\text{He}$  and H-minority regimes at  $B_T \approx 25$  kG and 17 kG, respectively, while the higher frequency provided heating in the H-minority and H-2nd harmonic regimes at  $B_T \approx 28$  kG and 14 kG, respectively. In the minority regimes a small percentage of a minority ion (H or  $^3\text{He}$ ) was added to the bulk ion species (D). The magnetic field was then set so that, at  $R \approx 132$  cm, the minority ion cyclotron motion was resonant with the RF at its fundamental frequency. In the second-harmonic regime the entire hydrogen ion population at  $R \approx 132$  cm was resonant at twice its fundamental cyclotron frequency. The RF power was coupled into the plasma via pairs of half-turn antennae. The other main parameters for these experiments were: major radius,  $R = 132$  cm; minor radius,  $a = 40$  cm; plasma current,  $I_p \leq 500$  kA; ICRF power,  $P_{RF} \lesssim 2$  MW; and line average electron density,  $\bar{n}_e \approx 2 \times 10^{13} \text{ cm}^{-3}$ . The main limiters [7] for these experiments were located at one toroidal position and were top-bottom carbon mushrooms and in-out 1/3-turn carbon rings. An auxiliary, movable, top-mounted carbon limiter was located  $100^\circ$  away toroidally in the counter clockwise direction as viewed from above. The LENS viewed the PLT plasma through the midplane at the same toroidal location as the auxiliary limiter.

Measurements were made during D- $^3\text{He}$  and H-D operation. The data shown are for D- $^3\text{He}$  but similar results occurred for both. This choice avoids confusion in interpreting the LENS time-of-flight signal, since only  $D^0$  is abundantly emitted from D- $^3\text{He}$  plasmas.

The evolution of the neutral emission,  $\Gamma$ , integrated over the energy range 25–1000 eV, is shown in Fig. 1 for three discharges: two with, and the third without, ICRF heating. In cases A and B, the auxiliary limiter was withdrawn from the plasma to  $r \approx 50$  cm. For

\* Present address: University of Illinois, Urbana, Illinois, 61801.

\*\* Present address: Mission Research Corporation, Albuquerque, New Mexico, 87106.

case C the auxiliary limiter was inserted to  $r = 40$  cm. For cases A and B the initiation and termination of the discharges are identical. The initiation and termination are also similar to the thousands of other Ohmically heated discharges monitored by the LENS. A major difference is seen during the application of ICRF power. The total flux increases sharply, a factor of five in  $200 \mu\text{s}$ . The flux remains approximately constant at the higher level throughout this ICRF heating pulse.

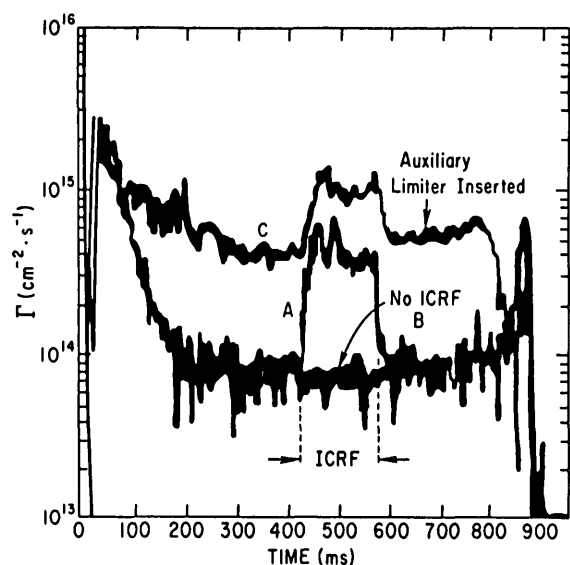


FIG.1. Flux of charge-exchange particles: A and B – at a position away from the limiters; C – at a position near an auxiliary limiter.

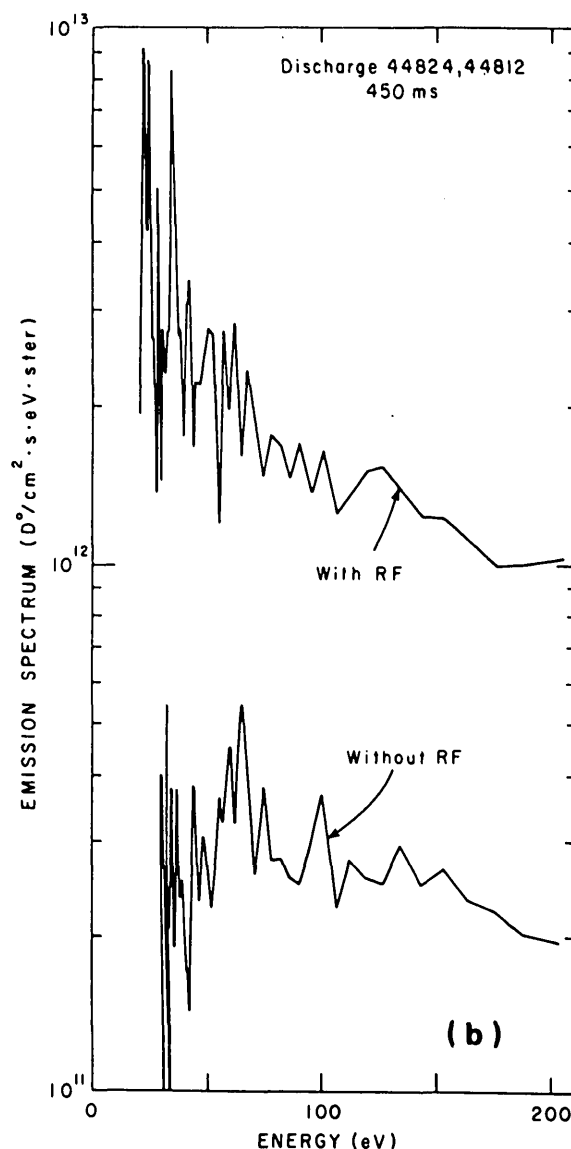
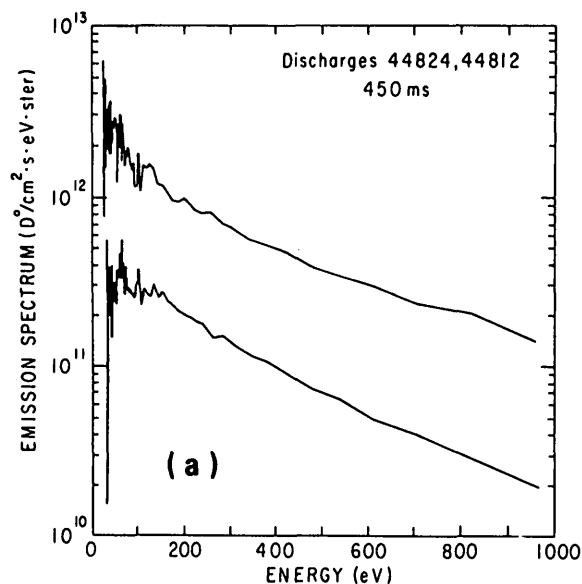


FIG.2. Flux spectra,  $d\Gamma/dE$ , with and without ICRF heating. (a) Energy range is 20–1000 eV; (b) energy range is 20–200 eV.



At the end of the ICRF heating pulse,  $\Gamma$  drops a factor of five in 1 ms. The line-averaged electron density was about  $2 \times 10^{13} \text{ cm}^{-3}$  before the about 150 ms long ICRF heating pulse. During the pulse it rose about 30%. Programming  $\bar{n}_e$  to behave in this fashion (without ICRF) resulted in no change to the LENS signal [8]. Also, puffing gas into the vessel near the antennae (but without ICRF applied) resulted in no increase in  $\Gamma$ . These measurements exclude the rise in  $n_e$  and gas desorption from the antennae as causes of the increase in  $\Gamma$ .

There are also cases where, though the ICRF power is constant, the high flux drops by about 50% during

the ICRF pulse. This may be due to impurity influx which is known [9] to reduce the charge-exchange  $D^{\circ}$  outflux. During these cases, when  $\Gamma$  drops during the ICRF pulse, impurity radiation, particularly from carbon, was seen to increase [10].

As shown in Fig. 2, the rise in  $\Gamma$ ,  $\Delta\Gamma$ , is not uniform across the measured energy range. A proportionally higher  $\Gamma$  is seen at  $25 < E < 50$  eV than at  $50 < E < 500$  eV. The average energy,  $\bar{E}$ , of the particles detected by the LENS drops during the first 50 ms of the ICRF by up to 25% of its initial value near 300 eV. The average energy recovers to about 300 eV over the next 100 ms. The flux spectra shown in Fig. 2 are averages over  $t = 250 \rightarrow 350$  ms (before ICRF) and  $t = 450 \rightarrow 550$  ms (during ICRF). They cannot be fit by single-temperature Maxwellians.

The flux spectra,  $d\Gamma/dE$ , have been modelled using two codes, DEGAS [11] and NEFRIT [12]. DEGAS calculates the neutral-density profiles in 3-D using  $T_e(r)$  and  $n_e(r)$  from Thomson scattering and a realistic wall model which includes atomic hydrogen reflection and implantation, and molecular hydrogen desorption. The code includes both limiter and wall processes in recycling. NEFRIT calculates the flux spectra given  $T_e(r)$  and  $n_e(r)$  from Thomson scattering and  $n_n(r)$  from DEGAS. The free parameter  $T_i(r)$  is used to fit the calculated  $d\Gamma/dE$  with the experimental one. Several iterations of DEGAS $\rightarrow$ NEFRIT $\rightarrow$ EXPERIMENTAL  $d\Gamma/dE$  are required to find  $T_i(r)$ . The experimental  $d\Gamma/dE$  (Fig. 2a and 2b), when interpreted with the realistic wall model in DEGAS, shows a drop in the edge ion temperature during ICRF heating from about 75 eV to less than about 25 eV. The edge is defined as the radial location where the neutral density peaks. This edge,  $a_{cx}$ , occurs at about  $r = (0.9 \pm 0.05)a$ . The error bars arise from the uncertainty in the energy of the recycling hydrogen. Cold recycling hydrogen (1/40 eV  $H_2$ ) would cause  $a_{cx} \cong 0.95 a$  and hot recycling hydrogen (500 eV  $H^{\circ}$ ) would cause  $a_{cx} \cong 0.85 a$ . The determination of  $T_i(r)$  depends on the wall model. In the unlikely event that the recycling hydrogen is all 1/40 eV atomic hydrogen, rather than the  $\approx 50/50$  mix of  $\approx 50$  eV atomic hydrogen and 1/40 eV molecular hydrogen (the approximate results of the DEGAS model), the experimental  $d\Gamma/dE$  during ICRF would also be consistent with the same edge temperature, 75 eV, as before the ICRF.

The increase in  $D^{\circ}$  efflux,  $\Delta\Gamma$ , was measured as a function of ICRF power. Up to about 1.5 MW,  $\Delta\Gamma$  increased linearly with applied power (Fig. 3a) at a rate of  $4 \times 10^{14} \text{ cm}^{-2} \cdot \text{s}^{-1} \cdot \text{MW}^{-1}$  for a plasma current of 520 kA. H-D plasmas generally showed a twice

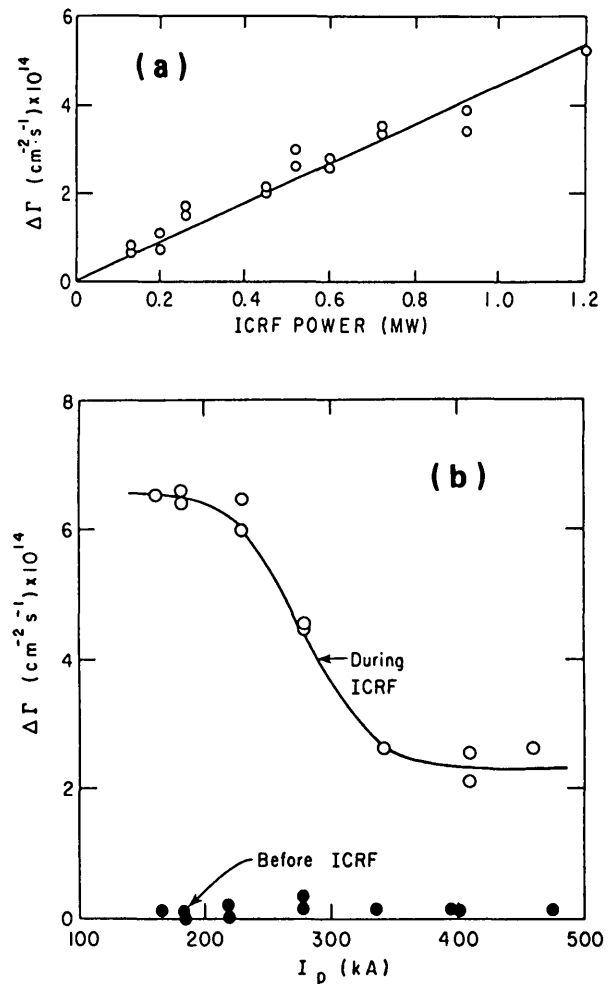


FIG.3. Change in flux,  $\Delta\Gamma$ : (a) versus applied ICRF power; (b) versus plasma current  $I_p$ , for an applied power of 520 kW. For both, the 25 MHz ICRF coil system was used for heating a  $D\text{-}^3\text{He}$  plasma.

higher rate than  $D\text{-}^3\text{He}$  plasmas. Above 2 MW there was a tendency for  $\Delta\Gamma$  to saturate.

The variation of  $\Delta\Gamma$  with plasma current was determined for the range  $150 < I_p < 500$  kA.  $\Delta\Gamma$  increased with decreasing current. The variation was sigmoidal in shape (Fig. 3b) with the point of inflection at about 300 kA. Ohmically heated plasmas show no variation in  $\Gamma$  with  $I_p$ , i.e.  $\Delta\Gamma < 10^{13} \text{ cm}^{-2} \cdot \text{s}^{-1}$ . It is interesting to note that the quality of ICRF heating improves with increasing plasma current [13].

Inserting the auxiliary limiter into PLT results in a reduction of about 25% of the power to the other limiters. It also causes up to a 30-fold increase in  $\Gamma$  seen by the LENS, depending on the minor radius of the auxiliary limiter. From considering DEGAS simulations, we note that even more severe poloidal

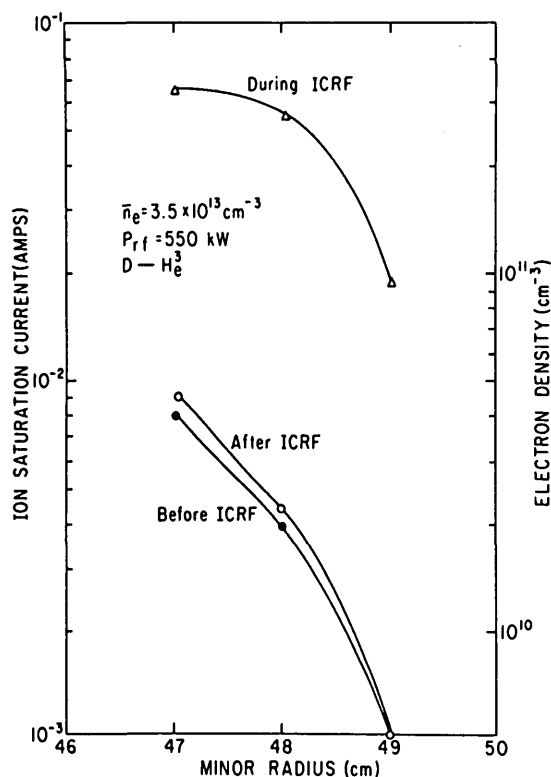


FIG. 4. Plasma density near the wall determined from ion saturation currents measured with a Langmuir probe.

asymmetries probably exist. Case C in Fig. 1 shows  $\Gamma$  for an ICRF-heated discharge with the auxiliary limiter inserted. For this case, a 5-fold increase in  $\Gamma$  was seen in the steady-state (150–400 ms) portion of the discharge before ICRF. However,  $\Delta\Gamma$  is the same as for case B, showing that  $\Delta\Gamma$  is approximately independent of proximity to the limiter.

Langmuir probe measurements were performed in the plasma about 3–10 cm outside the limiter radius. Electron density profiles, determined from the ion saturation current, are shown in Fig. 4 for three different times in an ICRF heated discharge. The electron density is seen to rise about a factor of ten. The scrape-off distance does show a tendency to lengthen, as noted earlier [14]. Little change is discernible in the electron temperature in this region, partially because of pick-up of 'noise' from the ICRF.

On the basis of the LENS and Langmuir probe data we propose that the following sequence of events occurs during ICRF heating: the application of ICRF power increases the radial transport of plasma, thereby raising the edge ion density at the wall. The hydrogen ions impinge on the wall. With about 50% probability they are immediately reflected, being

neutralized in the process. The other 50% are implanted in the wall at a depth of about 10 Å. They diffuse back to the surface, recombine into molecules and desorb from the surface. All this occurs in a few milliseconds. Both atomic and molecular neutrals enter the plasma and enhance the charge-exchange rate. Thus the underlying cause of  $\Delta\Gamma$  is a rise in the hydrogen ion density, at the wall,  $n_i(w)$ . The required increase in  $n_i(w)$  to give the large increase in  $\Gamma$  is small. It can be estimated by using the usual [7, 15] radial transport velocity of the edge plasma,  $v_r \approx 10^4 \text{ cm} \cdot \text{s}^{-1}$ . Then

$$\Delta n_i(w) \cong \Delta\Gamma/v_r \cong 10^{11} \text{ cm}^{-3} \quad (1)$$

which is about that seen by the Langmuir probes. The mechanisms which could cause an increased transport of protons to the edge include electron plasma waves (perhaps generated in the near-field region of the antennae), cyclotron resonances, stochastic transport, turbulence, or plasma potentials set up by the loss of energetic ions. The relative importance of these cannot yet be determined, though the time history of  $\Gamma$  and its independence on species heated may be useful for future evaluations of these mechanisms.

That *radial* transport of the main plasma is increased is speculative because there are several other means for increasing both the ion density in the scrape-off and the flux to the wall. Consider the particle conservation equation describing the number of particles in the scrape-off layer  $N_{so}$ ,

$$\dot{N}_{so} = \int dV \left( S - \frac{n_{sc}}{\tau_{\parallel}} \right) + \int dA (\Gamma_{in} - \Gamma_{out}) \quad (2)$$

where  $n_{so}$  is the ion density in the scrape-off,  $S$  is the birth rate by ionization of ions in the scrape-off,  $\Gamma_{in}$  is  $D_{\perp} \nabla n|_{r=a}$ ,  $\Gamma_{out} = D_{\perp} \nabla n|_{r=wall}$  and  $\tau_{\parallel}$  is the parallel confinement time (loss to the limiter). Estimates show  $S$  to be unimportant. For  $\Gamma_{out}$  to increase, either  $\tau_{\parallel}$  or  $\Gamma_{in}$  must increase, i.e. either radial confinement must degrade or parallel confinement must improve. We have not been able to measure changes in plasma flow to the limiter with sufficient accuracy to choose which changes,  $\tau_{\parallel}$  or  $\Gamma_{in}$ .

A drop in  $T_i(a)$  is beneficial since it reduces sputtering and desorption of impurities from the wall by the charge-exchange outflux. However, the increase in the charge-exchange outflux more than compensates for the drop in  $T_i$ , as far as charge-exchange sputtering is concerned. Calculations employing the detailed  $d\Gamma/dE$

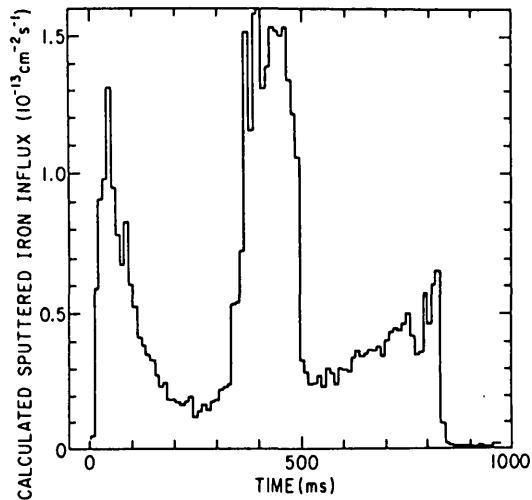


FIG. 5. Calculated sputtering of iron caused by the outflux of charge exchange  $D^0$  during an ICRF heated  $D-^3\text{He}$  discharge. The plasma parameters were  $\bar{n}_e = (2-3) \times 10^{13} \text{ cm}^{-3}$ ,  $I_p = 500 \text{ kA}$ , and  $P_{RF} = 1.2 \text{ MW}$ .

and the standard sputtering yields [16] show that the iron sputtered from the vessel wall should increase a factor of five to about  $1.2 \times 10^{13} \text{ MW}^{-1} \cdot \text{cm}^{-2} \cdot \text{s}^{-1}$  (see Fig. 5). For an impurity confinement time equal to the energy confinement time,  $\approx 20 \text{ ms}$ , this is adequate to explain the increases in iron seen [17] in the plasma during ICRF. However, the reduction in  $T_{i(a)}$  may be beneficial in reducing ion sputtering from the limiter since the density at  $r = a$  changes little.

The first effect of an increase in edge hydrogen recycling and its associated impurity influx would be electron cooling, primarily by radiation. Using the recent compilation by Janev et al. [18], radiative cooling due to enhanced toroidally symmetric hydrogen recycling during ICRF is estimated to be only  $\approx 5 \text{ kW} \cdot \text{MW}^{-1}$ . This is small compared to impurity radiation from the sputtered particles. Ion cooling results from either a change in ion thermal conductivity,  $\chi_i$ , or enhanced charge exchange. Coupling of the ions to the electrons at the edge is relatively unimportant. From calculations of hydrogen reflection from surfaces and the measured  $\Delta\Gamma$ , power loss from the ions due to the enhanced charge exchange is estimated to be about  $25 \text{ kW} \cdot \text{MW}^{-1}$  of ICRF heating in  $D-^3\text{He}$ . This could account for part of the observed ion cooling, though changes in  $\chi_i$  and a detailed analysis of electron-ion coupling across the entire profile must also be considered. The change in particle confinement, as ascertained by  $\Delta\Gamma/\Gamma$ , is not very large because of the severe poloidal asymmetry. The DEGAS calculations

and LENS data show that during the OH portion of the discharge, recycling at the limiter is 16 times more rapid than over the entire vacuum vessel. This ratio drops to 3:1 during ICRF heating of  $D-^3\text{He}$  at 1 MW.

In summary, we have discovered a rapid increase in hydrogen charge-exchange efflux that occurs with the application of ICRF power to PLT. This increased efflux is caused by an increase in ion density near the vacuum vessel wall. The physical mechanism responsible for this increase is not known. The efflux has a negative correlation with heating efficiency as a function of plasma current, i.e. low heating efficiency and high efflux both occur at low plasma currents. The efflux increases linearly with ICRF input power. The resultant wall sputtering and hydrogen recycling are estimated to affect substantially the electron and ion temperatures in the edge, the former by impurity radiation, the latter by charge-exchange thermalization.

## REFERENCES

- [1] HOSEA, J.C., BRETZ, N., CAVALLO, A., COLESTOCK, P., DAUGHNEY, C., et al., in Heating in Toroidal Plasmas (Proc. 3rd Joint Varenna-Grenoble International Symp. Grenoble, 1982), Vol. 1, Commission of the European Communities, Brussels (1982) 213.
- [2] TAKAHASHI, H., DAUGHNEY, C.C., ELLIS, R.A., Jr., GOLDSTON, R.J., HSUAN, H., NAGASHIMA, T., PAOLONI, F.J., SIVO, A.J., SUCKEWER, S., Phys. Rev. Lett. **39** (1977) 31.
- [3] SUCKEWER, S., HAWRYLUK, R.J., Phys. Rev. Lett. **40** (1978) 1649.
- [4] VOSS, D.E., COHEN, S.A., Rev. Sci. Instrum. **53** (1982) 1696.
- [5] RUZIC, D., COHEN, S., DENNE, B., SCHIVELL, J., J. Vac. Sci. Technol. A **1** (1983) 818.
- [6] MANOS, D.M., BUDNY, R., SATAKE, T., COHEN, S.A., J. Nucl. Mater. **111&112** (1982) 130.
- [7] COHEN, S.A., BUDNY, R., McCracken, G.M., ULRICKSON, M., Nucl. Fusion **21** (1981) 233.
- [8] VOSS, D.E., Low Energy Neutral Atom Emission and Plasma Recycling in the PLT Tokamak, Ph. D. Thesis, Princeton University (1981).
- [9] COHEN, S.A., CECCHI, J., DAUGHNEY, C., DAVIS, S., DIMOCK, D., et al., J. Vac. Sci. Technol. **20** (1982) 1226.
- [10] DENNE, B., private communication (1982).
- [11] HEIFETZ, D., POST, D.E., Comput. Phys. Commun. **29** (1983) 287.
- [12] RUZIC, D.N., Total Scattering Cross-sections and Interatomic Potentials for Neutral Hydrogen and Helium on Some Noble Gases, Ph. D. Thesis, Princeton University (1984).
- [13] HOSEA, J., ARUNASALAM, V. BERNABEI, S., BOYD, D., BRETZ, N., et al., Proc. School on Plasma Physics, Varenna (1979), Vol. 2, Commission of the European Communities, Brussels (1979) 571.

- [14] HSUAN, H., HAWRYLUK, R.J., SUCKEWER, S., TAKABASHI, H., in RF Plasma Heating (Proc. 3rd Conf. Pasadena, 1978) (unpublished), paper C8.
- [15] STRACHAN, J., et al., Nucl. Fusion 22 (1982) 1145.
- [16] BOHDANSKY, J., ROTH, J., BAY, H.L., J. Appl. Phys. 51 (1980) 2861.
- [17] STRATTON, B.C., MOOS, H.W., HODGE, W.L., SUCKEWER, S., HOSEA, J., HULSE, R., HWANG, D., WILSON, R., Nucl. Fusion 24 (1984) 767.
- [18] JANEV, R.K., POST, D.E., LANGER, W.D., EVANS, K., HEIFETZ, D.B., WEISHEIT, J.C., Survey of Atomic Processes in Edge Plasmas, Princeton Plasmas Physics Laboratory Rep. PPPL-2045 (1983).

(Manuscript received 23 July 1984  
Final manuscript received 26 September 1984)

### EQUILIBRIUM CONFIGURATIONS OF REVERSE FIELD PINCH PLASMA WITH A HELICAL MAGNETIC AXIS

N. TAKEUCHI, Y. KONDOH\*, T. SHIMADA\*\*, K. SUGITA\*\* (Department of Electrical Engineering, Tohoku University, Sendai, Japan)

**ABSTRACT.** A reverse field pinch (RFP) equilibrium configuration with helical magnetic axis is studied numerically over a wide range. The Grad-Shafranov equation is solved under the condition that the current flows along the magnetic field and the ratio of current to magnetic field is constant on every magnetic surface. Nested magnetic surfaces in the RFP are realized in this system; they are similar to those in a simple toroidal system. According to the direction of the helical winding, quite different RFP configurations are realized, depending on whether the current is parallel or antiparallel to the magnetic field. In the antiparallel case, the total plasma current is smaller than in the axisymmetric case although the ratio of current density to magnetic field is the same in both cases.

The reverse field pinch (RFP) configuration differs from the early toroidal pinches in that it has a special toroidal field of opposite directions inside and outside the plasma column [1].

The RFP configuration obtained in many experiments [2–5] agrees with what is predicted by theory.

\* Department of Electronic Engineering, Gunma University, Kiryu 376, Japan.

\*\* Department of Electrical Engineering, Iwate University, Morioka 020, Japan.

Experimentally, sufficiently high plasma density and temperature are realized. However, the most important problem to be solved is that there occurs a 'termination', i.e. the RFP configuration collapses abruptly after some time, so that plasma confinement is limited. Therefore, we are forced to investigate a more appropriate RFP configuration in a wider range of parameters. So far, RFP configurations were investigated in an axisymmetric system, in a simple toroidal system and in a system with helical conductors, Ohte [6, 7].

In this letter, we propose an RFP configuration system with non-planar magnetic axis. Many theoretical [8–10] and experimental studies of systems with non-planar axes were carried out in the past. However, most of this work concerns low-beta systems such as Vintotron [11], Asperator [12], and Heliac [13]. On the other hand, high-beta systems were not examined experimentally, except for Syllac [14], Isar [15], and Asperator-K [16]. Systems with non-planar magnetic axes are mainly divided into two types, one with helically symmetric axis [11–16] and the other one with an axis having inflection points [17–19]. The former system can simply be treated as two-dimensional, because of its helical symmetry. In this letter, we only treat this type; the latter system will be examined later.

To describe the various equilibria, we introduce a new set of co-ordinates attached to the helical axis. A Grad-Shafranov equation can be derived for those systems where the applied external magnetic fields have the same helical wavelength and the same helical axis as the co-ordinate system. In contrast to an axisymmetry system, two parameters are needed for the present analysis, i.e. the torsion and the curvature of the magnetic axis; the Grad-Shafranov equation can